Full Length Research Article

© 2026, Centre for Advanced Research in Agricultural Sciences
Research Journal of Agricultural Sciences
Volume 17; Issue 02 (Mar–Apr 2026); pp 146–152

ISSN: 0976-1675 (P)
ISSN: 2249-4538 (E)

Comparative Morphometry of Pupal Stages of *Bemisia tabaci* Infesting Brinjal (*Solanum melongena*) Across Agro-ecological Units of Kerala, India

S. R. Reshma[1], M. T. Ranjith*[1], Mani Chellappan[1], E. R. Harish[2], C. V. Vidya[1] and A. G. Kiran[3]

[1] Department of Agricultural Entomology, College of Agriculture, Vellanikkara, KAU, P. O., Thrissur - 680 656, Kerala, India
[2] Division of Crop Protection, ICAR- Central Tuber Crops Research Institute, Sreekaryam, Thiruvananthapuram, Kerala India
[3] Centre for Plant Biotechnology and Molecular Biology, College of Agriculture, Vellanikkara, KAU, P. O., Thrissur - 680 656, Kerala, India

Received: 09 Nov 2025; Revised accepted: 28 Feb 2026

Abstract

The tobacco whitefly, *Bemisia tabaci*, is a major global pest, and its complex nature poses significant challenges to agriculture, particularly in its role as a vector for severe plant viruses like Brinjal yellow mosaic virus (BYMV). In Kerala, India, this pest severely impacts brinjal (*Solanum melongena*) cultivation, an economically vital crop. Recognizing the pest's reported high morphological plasticity and the existence of cryptic species, this study aimed to characterize the intraspecific morphological variability of *Bemisia tabaci* pupae collected from brinjal plants across seven diverse agro-ecological units (AEUs) in Kerala. Using standard clearing, staining, and mounting techniques, fifteen key puparial morphometric traits were measured and analyzed across fourteen districts of Kerala. While initial observations showed subtle differences in overall dimensions, Principal Component Analysis (PCA) effectively revealed significant population segregation. The first two principal components (PC1 and PC2) collectively explained 75.3% of the total variance. PC1 was strongly driven by pupal width (PW), operculum length (OL), and lingula length (LL), clearly separating populations of Wayanad and Ernakulam as having distinct, larger pupal size-related features. PC2, on the other hand, was influenced by wax margin dimensions (LRWM, LLWM) and vasiform orifice length (VOL), highlighting populations Kottayam, Idukki and Palakkad. These results confirm the existence of distinct morphotypes within *Bemisia tabaci* infesting brinjal in Kerala, suggesting that local environmental conditions, host plant factors, and micro-climatic variation are driving phenotypic differentiation. This structural diversity emphasizes the pest's high adaptability, underscoring the necessity for location-specific and integrated pest management strategies.

***Key words*:** *Bemisia tabaci*, Puparium, Brinjal, Morphometries, Multivariate analyses

The tobacco whitefly, *Bemisia tabaci* (Gennadius) (Hemiptera: Aleyrodidae), is regarded as one of the most devastating invasive pests threatening global agricultural production. Its extensive geographical distribution is primarily facilitated by the international movement of infested plant materials through trade and transport systems. Once introduced into a new ecosystem, *Bemisia tabaci* establishes rapidly and proliferates, causing direct damage by extracting phloem sap thereby resulting in plant weakening and indirect damage by acting as an efficient vector for numerous plant viruses [1]. In India, *Bemisia tabaci* was initially reported from cotton fields in Punjab in 1905 [2]. Since then, the pest has become prevalent across tropical and subtropical regions where climatic conditions favor its growth and reproduction. Over time, several biotypes or cryptic species within the *Bemisia tabaci* complex have been identified, displaying marked variability in characteristics such as host plant preference, virus transmission capability, and insecticide resistance [3]. These inter-population variations pose significant challenges for management, as control measures effective against one biotype may not be suitable for others. Presently, *Bemisia tabaci* ranks among the most serious invasive pest species impacting global agriculture. Its persistent spread and high adaptability emphasize the necessity for robust, integrated pest management (IPM) approaches that combine continuous surveillance, utilization of resistant crop genotypes, application of biological control agents, and rational use of chemical pesticides [4-6].

Brinjal (*Solanum melongena* L.), commonly known as eggplant, is an economically important vegetable crop cultivated widely across Kerala, both in kitchen gardens and under commercial production systems. It plays a crucial role in the state's agricultural economy and dietary diversity, being a rich source of fiber, vitamins, and minerals. However, brinjal cultivation faces considerable challenges due to infestations by insect pests and the spread of viral diseases, among which the whitefly, *Bemisia tabaci* (Gennadius), has emerged as a predominant pest. High levels of infestation have been reported from major brinjal-growing regions such as Palakkad, Thrissur,

***Correspondence to:** M. T. Ranjith, E-mail: ranjith.mt@kau.in; Tel: +91 6238347587

Citation: Reshma SR, Ranjith MT, Chellappan M, Harish ER, Vidya CV, Kiran AG. 2026. Comparative morphometry of pupal stages of *Bemisia tabaci* infesting brinjal (*Solanum melongena*) across agro-ecological units of Kerala, India. *Res. Jr. Agril. Sci*. 17(2): 146-152.

Idukki, and Wayanad [7]. The pest inflicts direct damage through phloem sap extraction, resulting in chlorosis, leaf curling, and stunted growth, while the honeydew excreted promotes the development of sooty mould, further reducing photosynthetic efficiency. More critically, *Bemisia tabaci* serves as a highly efficient vector of several begomoviruses, including the *Brinjal yellow mosaic virus* (BYMV) and *Tomato leaf curl New Delhi virus* (ToLCNDV), both of which are responsible for severe yield losses and quality deterioration in brinjal crops [8-9]. The increasing prevalence of these whitefly-transmitted viral diseases underscores the urgent need for integrated pest and disease management strategies to sustain brinjal production in the region.

Over the last two decades, extensive research has revealed that *Bemisia tabaci* exhibits far greater taxonomic complexity than previously recognized. De Barro *et al.* [1] demonstrated that *Bemisia tabaci* represents a cryptic species complex comprising at least 24 morphologically indistinguishable species, organized into 11 primary genetic lineages. This intricate diversity is largely attributed to the insect's highly polyphagous nature, enabling it to adapt successfully to a wide range of host plants and environmental conditions, thereby promoting substantial population-level differentiation, particularly within brinjal-growing regions. Historically, external morphological characteristics have been regarded as valuable and practical diagnostic tools for distinguishing whitefly species [10-11]. In support of this, Li *et al.* [12] reported that morphometric evaluation of puparial traits can effectively discriminate among *Bemisia tabaci* biotypes. In this context, the present study aims to characterize the morphological variability of *Bemisia tabaci* during the pupal stage across different agro-ecological zones of Kerala, with the goal of elucidating intraspecific diversity and potential patterns of population differentiation within this pest complex.

MATERIALS AND METHODS

Surveys were undertaken across seven agro-ecological units (AEUs 9, 10, 11, 12, 14, 21, and 23), covering all fourteen districts of Kerala. Whitefly puparia were collected from brinjal plants during the period from December 2024 to September 2025, and the collection details are summarized in (Table 1). Sampling involved manually excising leaves bearing fourth-instar nymphs (puparia), which were subsequently processed for morphometric examination.

The collected specimens were initially placed in watch glasses containing 10% potassium hydroxide (KOH) solution and kept overnight at ambient temperature to facilitate tissue clearing. After digestion, the internal contents were carefully expelled by applying gentle pressure, followed by rinsing in distilled water for approximately three minutes to remove any remaining potassium hydroxide (KOH) or debris. The cleared samples were then transferred into 80% ethanol for 10 minutes for dehydration.

Table 1 Details of survey carried out across various agro-ecological units of Kerala

Districts	Code	AEU	Latitude	Longitude	Elevation (above MSL)	Brinjal variety
Thiruvananthapuram	TVM (T_1)	9	8.473844°N	76.960905°E	68 m	Haritha
Kollam	KLM (T_2)	9,12	8.902715°N	76.800402°E	150 m	Local variety
Pathanamthitta	PTA (T_3)	9,12	9.419397°N	76.602196°E	18 m	Swetha
Alappuzha	ALP (T_4)	4	9.546097°N	76.324391°E	1 m	Haritha
Kottayam	KTY (T_5)	9,12	9.473765°N	76.555836°E	1.5 m	Local variety
Idukki	IDK (T_6)	14	9.908212°N	76.697291°E	40 m	Local variety
Ernakulam	ERN (T_7)	9	10.1926°N	76.3869°E	31 m	Local variety
Thrissur	TRS (T_8)	10,11	10.54907°N	76.281334°E	22.25 m	Haritha, Neelima
Palakkad	PLK (T_9)	10,11,23	10.63406°N	76.722523°E	78 m	Local variety
Malappuram	MLP (T_{10})	10,11	10.854714°N	75.989174°E	20 m	Local variety
Kozhikode	KKD (T_{11})	10,11	11.389135°N	75.755812°E	42 m	Local variety
Wayanad	WYD (T_{12})	21	11.609519°N	76.209791°E	1010 m	Surya
Kannur	KNR (T_{13})	10,11	12.0972°N	75.1934°E	38.78 m	Local variety
Kasargod	KSG (T_{14})	10,11	12.400152°N	75.080695°E	15 m	Local variety

Staining was carried out using acid fuchsin, with the specimens left in the stain overnight. Excess dye was removed by the addition of a drop of glacial acetic acid (GAA), and the specimens were subsequently rinsed in freshly prepared 80% ethanol for ten minutes. The stained puparia were then immersed in clove oil and left overnight to enhance transparency prior to mounting.

For slide preparation, a drop of clove oil was placed on pre-labelled microscope slides, and the specimens were gently positioned before covering with a cover slip to prevent air bubble formation. From each sampling location, five specimens were mounted and observed under a Leica DM100® phase-contrast microscope at 40× magnification to record key morphological features.

The measured puparial traits (Fig 1) included total body length and width, right and left anterior wax margin length and width, vasiform orifice length, operculum length and width, lingula length and width, caudal furrow length, caudal setae length, and the distance between caudal setae. The morphometric data were subjected to statistical analysis using one-way Analysis of Variance (ANOVA) in the RAISINS software to determine the extent of variation across the different AEUs.

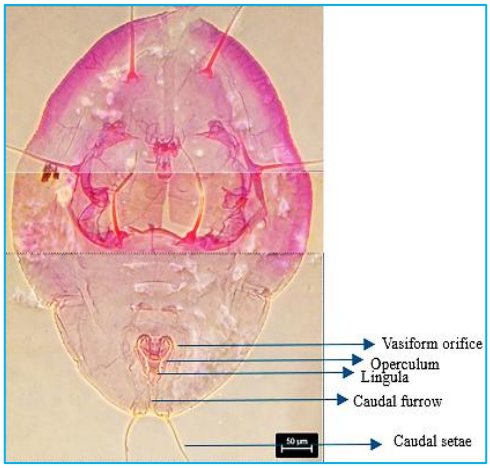

Fig 1 Fourth larval instar or puparium

RESULTS AND DISCUSSION

The morphometric observations of *Bemisia tabaci* pupae collected from brinjal grown across different agro-ecological regions of Kerala revealed slight, but consistent variations in body dimensions (Table 2). The data represent the mean of five observations for each parameter and location (T_1–T_{14}).

Pupal length (PL) and pupal width (PW)

The pupal length ranged between 0.70 mm and 0.72 mm, showing minor variation among the different samples. The highest length of 0.72 mm was recorded in T_{11}, suggesting slightly larger pupae in that region, possibly due to favourable host conditions or environmental suitability. The smallest pupae (0.70 mm) were noted in T_7 and T_{12}, indicating a comparatively restricted growth, which may be influenced by ecological or nutritional factors of the host leaves. The pupal width exhibited greater variability than the length, ranging from 0.47 mm to 0.58 mm. The widest pupae were recorded in T_7 and T_{12} (0.58 mm), indicating broader, well-developed individuals possibly adapted to those specific microclimatic conditions. Conversely, the narrowest pupae (0.47 mm) were noted in treatments T_1, T_2, T_3, T_4, T_{10}, and T_{14}, suggesting that in these locations, the pupae were slender, which could be an adaptive response to local stress or temperature conditions.

Length and width of right anterior wax margin (LRWM and WRWM)

The length of the right wax margin (LRWM) varied between 0.06 mm and 0.08 mm, with the highest value (0.08 mm) recorded in T_4, T_5, T_6, T_9, and T_{11}, indicating more pronounced wax margin development in these regions. The width (WRWM) remained stable at around 0.02 mm, with slight increases to 0.03 mm in T_4, suggesting minor structural thickening in that population. The development of the wax margin plays a protective role, and these small variations might reflect environmental adaptation to humidity or pest pressure.

Length and width of left anterior wax margin (LLWM and WLWM)

Similar to the right side, the length (LLWM) ranged from 0.06 mm to 0.08 mm, with higher values again in T_4, T_5, T_6, T_9, and T_{11}. The width (WLWM) varied slightly between 0.02 mm and 0.02d, with thicker margins noted in T_5, T_6, T_7, T_9, and T_{12}. The relatively symmetrical values between the right and left sides indicate a balanced morphological growth pattern in most populations.

Vasiform orifice length (VOL)

The vasiform orifice length was consistent across treatments, averaging 0.07 mm, with only slight differences noted in T_5, T_6, and T_9 (0.07a). This stability indicates that this structure, which plays a role in excretion and respiration, remains morphometrically conservative across ecological regions.

Operculum length (OL) and width (OW)

The operculum length (OL) ranged between 0.03 mm and 0.04 mm, while the width (OW) remained stable at 0.04 mm for all treatments. The largest OL (0.04 mm) was noted in T_7 and T_{12}, suggesting slightly longer opercula in those populations. Such uniformity across regions indicates that operculum dimensions are a stable taxonomic feature of the species, with minor localized variations.

Table 2 Mean of five observations

	PL	PW	LRWM	WRWM	LLWM	WLWM	VOL	VOW	OL	OW	LL	LW	CFL	CSL	DCS
T_1	0.71^{b}	0.47^{e}	0.07^{d}	0.02^{a}	0.07^{d}	0.02^{b}	0.07^{b}	0.05^{a}	0.03^{b}	0.04	0.05^{c}	0.02^{a}	0.05^{a}	0.09^{a}	0.04^{a}
T_2	0.71^{b}	0.47^{e}	0.07^{d}	0.02^{a}	0.07^{d}	0.02^{b}	0.07^{b}	0.05^{a}	0.03^{b}	0.04	0.05^{c}	0.02^{a}	0.05^{a}	0.09^{a}	0.04^{a}
T_3	0.71^{b}	0.47^{e}	0.07^{d}	0.02^{a}	0.07^{d}	0.02^{b}	0.07^{b}	0.05^{a}	0.03^{b}	0.04	0.05^{c}	0.02^{a}	0.05^{a}	0.09^{a}	0.04^{a}
T_4	0.71^{c}	0.47^{e}	0.08^{b}	0.03^{a}	0.08^{b}	0.02^{a}	0.07^{b}	0.05^{b}	0.03^{bc}	0.04	0.05^{b}	0.02^{c}	0.05^{c}	0.08^{b}	0.04^{a}
T_5	0.71^{c}	0.49^{c}	0.08^{b}	0.02^{b}	0.08^{b}	0.02^{d}	0.07^{a}	0.05^{b}	0.03^{ab}	0.04	0.05^{c}	0.02^{c}	0.05^{b}	0.09^{a}	0.04^{b}
T_6	0.71^{c}	0.49^{c}	0.08^{b}	0.02^{b}	0.08^{b}	0.02^{d}	0.07^{a}	0.05^{b}	0.03^{ab}	0.04	0.05^{c}	0.02^{c}	0.05^{b}	0.09^{a}	0.04^{b}
T_7	0.70^{d}	0.58^{a}	0.06^{e}	0.02^{c}	0.06^{e}	0.02^{d}	0.07^{b}	0.05^{b}	0.04^{a}	0.04	0.06^{a}	0.02^{a}	0.05^{b}	0.09^{a}	0.04^{a}
T_8	0.71^{c}	0.49^{b}	0.07^{c}	0.02^{b}	0.08^{c}	0.02^{c}	0.07^{c}	0.05^{b}	0.03^{ab}	0.04	0.05^{b}	0.02^{ab}	0.05^{b}	0.08^{b}	0.04^{a}
T_9	0.71^{c}	0.49^{c}	0.08^{b}	0.02^{b}	0.08^{b}	0.02^{d}	0.07^{a}	0.05^{b}	0.03^{ab}	0.04	0.05^{c}	0.02^{c}	0.05^{b}	0.09^{a}	0.04^{b}
T_{10}	0.71^{b}	0.47^{e}	0.07^{d}	0.02^{a}	0.07^{d}	0.02^{b}	0.07^{b}	0.05^{a}	0.03^{b}	0.04	0.05^{c}	0.02^{a}	0.05^{a}	0.09^{a}	0.04^{a}
T_{11}	0.72^{a}	0.47^{d}	0.08^{a}	0.02^{b}	0.08^{a}	0.02^{c}	0.07^{b}	0.05^{a}	0.03^{c}	0.04	0.05^{c}	0.02^{b}	0.05^{a}	0.08^{b}	0.04^{b}
T_{12}	0.70^{d}	0.58^{a}	0.06^{e}	0.02^{c}	0.06^{e}	0.02^{d}	0.07^{b}	0.05^{b}	0.04^{a}	0.04	0.06^{a}	0.02^{a}	0.05^{b}	0.09^{a}	0.04^{a}
T_{13}	0.71^{c}	0.49^{b}	0.07^{c}	0.02^{b}	0.08^{c}	0.02^{c}	0.07^{c}	0.05^{b}	0.03^{ab}	0.04	0.05^{b}	0.02^{ab}	0.05^{b}	0.08^{b}	0.04^{a}
T_{14}	0.71^{b}	0.47^{e}	0.07^{d}	0.02^{a}	0.07^{d}	0.02^{b}	0.07^{b}	0.05^{a}	0.03^{b}	0.04	0.05^{c}	0.02^{a}	0.05^{a}	0.09^{a}	0.04^{a}

Pupal length (PL), pupal width (PW), length (LRWM) and width (WRWM) of right anterior wax margin, length (LLWM) and width (WLWM) of left anterior wax margin, vasiform orifice length (VOL), operculum length (OL), operculum width (OW), lingula length (LL), lingula width (LW), caudal furrow length (CFL), caudal seta length (CSL) and distance between caudal setae (DCS)

Lingula length (LL) and width (LW)

The lingula length showed values between 0.05 mm and 0.06 mm, with longer measurements (0.06 mm) observed in T_7 and T_{12}. This may correspond with better-developed internal structures, possibly influenced by pupal size and developmental stage. The lingula width remained uniform at 0.02 mm, signifying limited morphological variability in this feature among regional populations.

Caudal furrow length (CFL)

The caudal furrow length was constant across population collected from all locations, maintaining a mean value of 0. 05 mm, indicating that this feature is morphologically conserved in *Bemisia tabaci* pupae regardless of environmental conditions or host variation.

Caudal seta length (CSL) and distance between caudal setae (DCS)

The caudal setae exhibited minor variation, with most treatments showing a value of 0.09 mm, except T_4 and T_8 which recorded slightly lower values (0.08 mm). Longer caudal setae may help in anchoring the pupa to the leaf surface, and these subtle differences could be ecological adaptations to leaf texture and moisture. The distance between caudal setae remained

constant across almost all treatments, averaging 0.04 mm, suggesting this parameter is relatively uniform among the studied populations and less influenced by ecological factors.

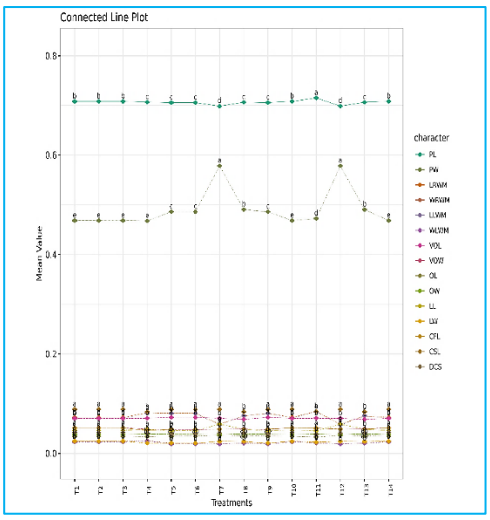

Fig 2 Connected line plot of pupal characters

Although the observed morphometric variations among treatments (T_1–T_{14}) were minor, they indicate micro-level morphological diversity in *Bemisia tabaci* pupae infesting brinjal across Kerala. The slight differences (Fig 2) in pupal width, wax margin dimensions, and caudal setae suggest environmental factors, host plant physiology, and local climatic conditions subtly influence pupal development. These variations highlight the species' adaptability to different ecological regions, an important aspect of its survival and distribution.

Principal component analysis

Principal components

PC1 accounts for approximately 42.58% of the variance in the dataset, while PC2 accounts for about 32.72% of the variance. Together, PC1 and PC2 explain approximately 75.3% of the total variance (termed as cumulative variance). Since PC1 explains more than 40% of the variance, a PC1-based index score is a strong consideration. Additionally, since both PCs explain more than 60% of the variance in the data, an index score based on both PCs is also appropriate. The correlation between each component is given in (Table 3).

Table 3 Principal components of fifteen variables present in *Bemisia tabaci* pupa

	PC1	PC2	PC3	PC4	PC5
Pupal length	-0.37	-0.09	0.01	0.29	-0.25
pupal width	0.37	0.1	0.05	0.09	-0.32
Length of right anterior wax margin	-0.36	0.2	-0.04	0.01	0.05
Width of right anterior wax margin	-0.23	-0.28	-0.07	-0.52	0.06
Length of left anterior wax margin	-0.35	0.21	-0.02	0.04	0.11
Width of left anterior wax margin	-0.23	-0.3	0.12	-0.40	-0.28
Vasiform orifice length	-0.04	0.19	-0.59	-0.16	-0.09
Vasiform orifice width	-0.13	-0.42	-0.04	0.16	-0.16
Operculum length	0.37	0.01	0.01	-0.08	0.50
Operculum width	-0.2	0.25	0.41	0.14	0.30
Lingula length	0.36	0.02	0.17	-0.09	-0.46
Lingula width	0.13	-0.4	0.16	0.26	0.06
Caudal furrow length	-0.08	-0.34	-0.22	0.52	0.08
Caudal seta length	0.15	-0.17	-0.54	-0.01	0.22
Caudal setae	0.05	-0.39	0.24	-0.23	0.31

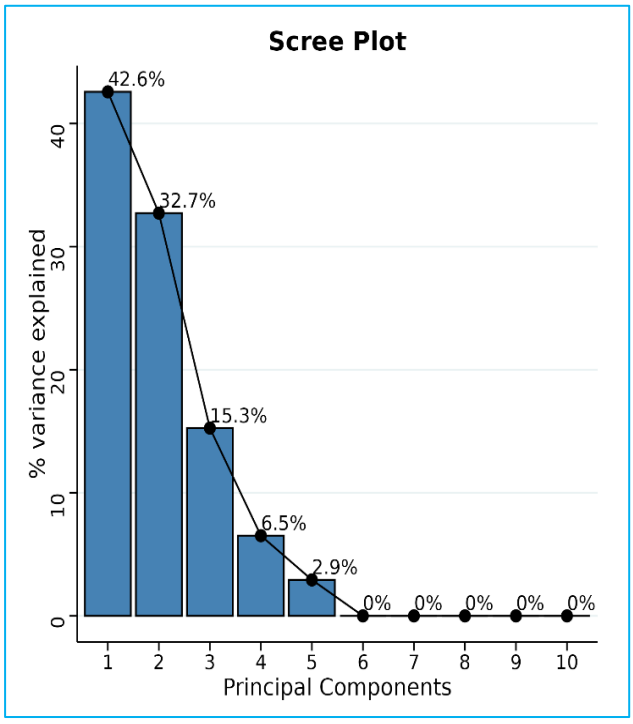

Fig 3 Scree plot of principal components

The scree plot (Fig 3) presented above reveals the percentage of variance explained by each principal component obtained through Principal Component Analysis (PCA). The first principal component (PC1) accounts for the highest proportion of total variance at 42.6%, indicating that it captures the largest amount of variation present in the dataset. The second component (PC2) explains 32.7% of the variance, which, when combined with PC1, represents a cumulative variance of approximately 75.3%. The third component (PC3) contributes an additional 15.3%, increasing the total variance explained to over 90% by the first three components. Subsequent components (PC4 to PC10) explain progressively smaller portions of variance, each contributing less than 7%, with the remaining components contributing negligibly (approaching 0%).

The sharp decline in the scree plot from PC1 to PC3, followed by a gradual leveling off, suggests that the first few principal components contain the most meaningful information, while the later components mainly represent random noise or minor variations within the data. This characteristic "elbow" shape of the scree plot typically indicates the optimal number of components to retain for further analysis. In this case, the distinct inflection point after the third component implies that three principal components are sufficient to explain the majority of variation in the dataset.

The index plot based on the first principal component (PC1) (Fig 4) illustrates the relative performance of the fourteen treatments (T_1–T_{14}) with respect to their PCA-scaled index values. This radial or circular plot helps visualize how each treatment contributes to the overall variation explained by PC1. The distance of each treatment point from the center represents its magnitude of contribution to the first principal component, with values closer to the outer edge indicating higher performance or stronger association with the key traits identified in the PCA.

From the plot, it is evident that treatments T_7 and T_{12} are positioned farthest from the origin, falling outside the red boundary circle and marked as "selected" treatments. This indicates that these two treatments have the highest PCA-scaled index values, implying superior performance in terms of the morphometric parameters that contributed most strongly to PC1. In contrast, the remaining treatments cluster closer to the center, showing relatively lower index values and therefore a lesser influence on the primary source of variation. The red circle in the plot represents the selection threshold, differentiating treatments with outstanding characteristics (selected) from those with moderate or lower responses (non-selected). Overall, the index plot demonstrates that treatments T_7 and T_{12} are distinctly superior when considering the traits that contributed significantly to PC1.

The index plot based on the second principal component (PC2) (Fig 5) illustrates the relative contribution of each treatment (T_1–T_{14}) to the variation captured by the second axis of the principal component analysis. From the plot, it is evident that treatments T_5, T_6, and T_9 lie beyond the red boundary, marking them as the most influential treatments under PC2. Their higher PCA-scaled index values suggest that these treatments express distinct morphometric characteristics that contribute substantially to the second principal component. In contrast, the other treatments cluster closer to the center, indicating relatively smaller or less significant contributions to PC2-related variability. The separation of selected and non-selected treatments highlights the existence of considerable morphological or structural diversity among the tobacco whitefly pupae under different treatments. Overall, the index plot demonstrates that treatments T_5, T_6, and T_9 represent the most prominent performers based on the traits influencing PC2.

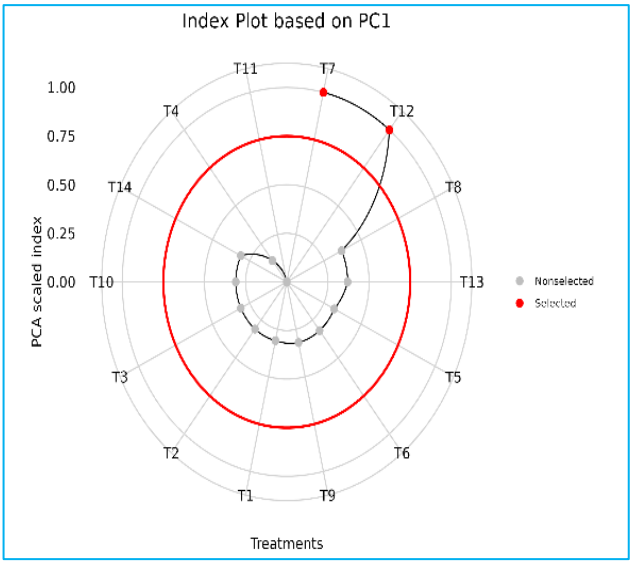

Fig 4 Index plot of principal component 1

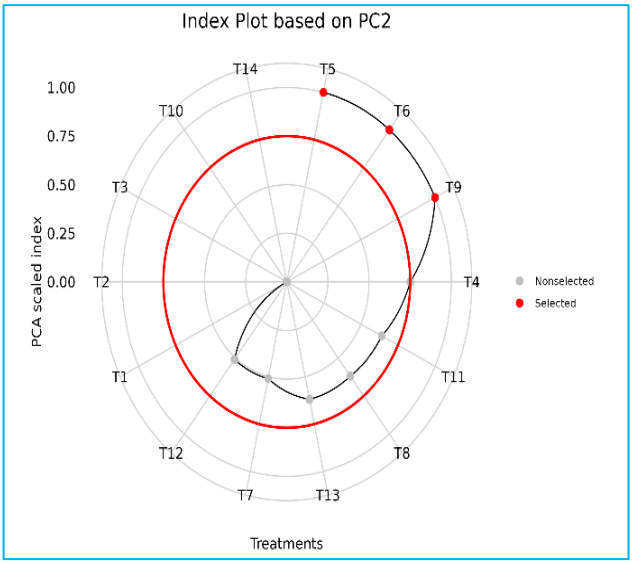

Fig 5 Index plot of principal component 2

Biplot analysis

The Principal Component Analysis (PCA) biplot (Fig 6) displays the relationship between the different treatments (T_1–T_{14}) and the measured morphometric parameters of *Bemisia tabaci* pupae on brinjal, based on the first two principal components, PC1 and PC2, which together explain 75.3% of the total variance (42.58% from PC1 and 32.72% from PC2). The arrows in the plot represent the original morphological variables, and their direction and length indicate the extent and nature of their contribution to each principal component. Treatments are plotted as points, showing how they group or separate according to their morphological similarities or differences.

The biplot reveals that PC1 is primarily influenced by traits such as pupal width (PW), operculum length (OL), and lingula length (LL), as indicated by the rightward orientation of their vectors. Treatments T_7(Ernakulam) and T_{12}(Wayanad), positioned on the positive side of PC1, are strongly associated with these parameters, suggesting that these treatments produced pupae with comparatively larger body width and better-developed operculum and lingula structures. On the other hand, PC2 is mainly associated with variables such as length and width of the right and left anterior wax margins (LRWM, LLWM, WRWM, WLWM) and vasiform orifice length (VOL), which point upward in the plot. Treatments T_5(Kottayam), T_6(Idukki), and T_9(Palakkad) are positioned along the positive PC2 axis, indicating that these treatments are characterized by more pronounced wax margin features and larger vasiform orifice dimensions.

Conversely, treatments located near the origin or in the lower quadrants, such as T_1, T_2, and T_{10}, show relatively lower associations with the major morphological traits, indicating that they contributed minimally to the overall variability in the data. The grouping and spread of the treatments across the four quadrants highlight distinct morphological patterns among the pupae, likely reflecting differences in the environmental or experimental conditions associated with each treatment.

Overall, the PCA biplot effectively summarizes the interrelationships among morphometric traits and treatments, demonstrating that T_7 and T_{12} are strongly associated with pupal size-related features, whereas T_5, T_6, and T_9 are more closely linked to wax margin and vasiform orifice characteristics. These findings align with the results of the scree and index plots, confirming that variation in pupal morphology is driven primarily by a few key traits and that certain treatments exert a stronger influence on these features than others.

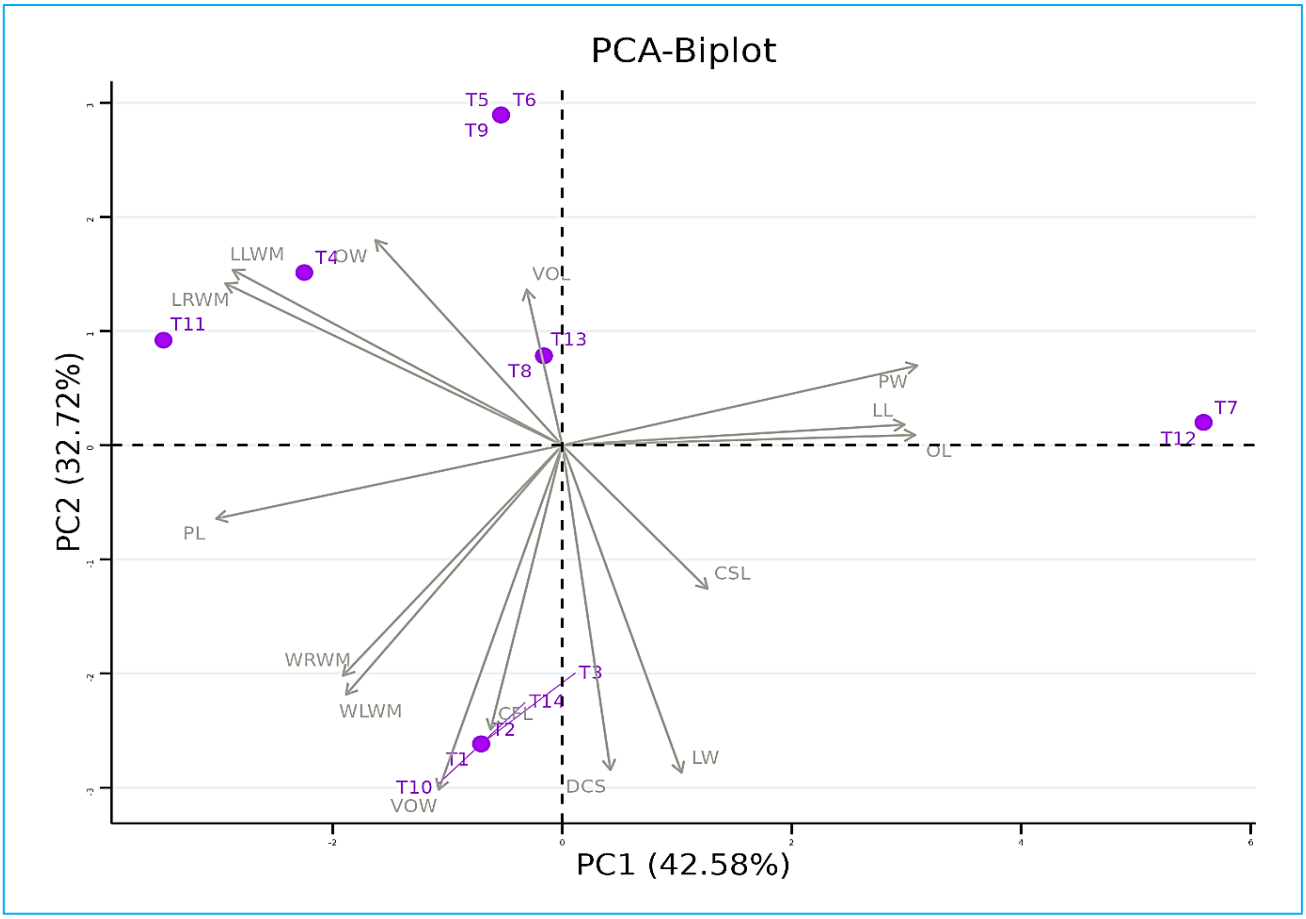

Fig 6 Biplot graph of principal components

The present study revealed significant morphometric variations in the pupal stages of *Bemisia tabaci* collected from brinjal across different agro-ecological units (AEUs) of Kerala. The analysis of 15 morphological characters using Principal Component Analysis (PCA) showed clear population segregation, indicating phenotypic diversity among whitefly populations. Such variations have also been reported in earlier studies, suggesting that the *B. tabaci* complex exhibits high morphological plasticity influenced by environmental conditions and host-plant factors [1], [12].

Among the 15 traits studied, width-related and structural characters such as as pupal width (PW), operculum length (OL), and lingula length (LL) contributed most significantly to the total variance. These features effectively discriminated the populations from different regions, as observed in the PCA biplot, where distinct clustering of populations such as those from Ernakulam and Wayanad was evident. Similar morphological differentiation among populations across agro-ecological zones was reported by Harish *et al*. [13], who found that variations in width and vasiform orifice characters served as reliable discriminators in *B. tabaci* populations infesting cassava.

Variations observed in pupal morphology may result from several influencing factors such as altitude, ambient temperature, host plant variety, and prevailing cultivation practices. Earlier studies have highlighted that host-associated morphological differences serve as important indicators of adaptive evolution within *Bemisia tabaci* populations [10], [14]. In the present study, populations from higher elevation regions like Wayanad (A.E.U. 21) and Idukki (A.E.U. 14) displayed greater pupal length but comparatively reduced pupal width, suggesting that environmental gradients particularly temperature and humidity may play a regulatory role in shaping pupal growth and form. These results corroborate the observations of Yan [11] and Li *et al.* [12], reported that puparial morphology is a reliable indicator of environmental adaptation in whiteflies.

The outcomes of this study also support the broader global understanding that *B. tabaci* constitutes a complex of cryptic species exhibiting marked intraspecific variation influenced by both host and habitat conditions [1], [15]. The detection of distinct morphotypes within tomato-growing areas of Kerala indicates that ecological and environmental heterogeneity may be driving microevolutionary differentiation among local populations. These morphological trends agree with molecular-level evidence presented by Peng *et al.* [14], who demonstrated that genetic structuring in *B. tabaci* often correlates with geographic and host-associated diversity.

In summary, the present study highlights that specific morphological attributes particularly those associated with the vasiform orifice and pupal width can serve as valuable markers for distinguishing intraspecific populations. Such phenotypic differentiation is of practical relevance, as it may influence virus transmission capacity and pest adaptability under varying climatic and crop conditions [16]. Therefore, integrating morphometric characterization with molecular analyses would provide a more comprehensive understanding of *B. tabaci* diversity and facilitate the formulation of precise, location-specific management strategies suited to Kerala's diverse agro-ecological systems.

CONCLUSION

The current study successfully characterized the morphological variations in the puparia stage of the tobacco whitefly, *Bemisia tabaci*, populations collected from brinjal across the diverse agro-ecological landscape of Kerala. The consistent, albeit minor, variations in traits like pupal width,

operculum length, and lingula length, which collectively drove the greatest variance in the Principal Component Analysis (PCA) demonstrate that *B. tabaci* exhibits significant micro-level morphological diversity in response to local ecological and host conditions. Our findings, particularly the clustering and separation revealed by the PCA biplot, support the broader scientific consensus that *B. tabaci* is a cryptic species complex with substantial intraspecific variation. The morphological differentiation observed, where populations form Ernakulam and Wayanad were distinguished by size-related features while others Kottayam, Idukki and Palakkad populations were characterized by wax margin attributes, highlights that different sets of traits are under varying selection pressures across Kerala's agro-ecosystems. This phenotypic plasticity is crucial for the whitefly's survival and adaptability, and it carries practical implications for management. Since distinct morphotypes may correlate with differences in virus transmission efficiency and resistance to certain pesticides, a uniform control strategy is likely to be ineffective. Therefore, the morphometric data generated here serves as a valuable baseline for future efforts. We strongly recommend integrating this morphological characterization with molecular studies (such as sequencing) to precisely identify the prevailing *B. tabaci* biotypes in each agro-ecological unit. This comprehensive approach is essential for developing robust, location-specific Integrated Pest Management (IPM) programs that can sustainably safeguard brinjal production in the region.

Acknowledgement

We acknowledge Department of Agricultural Entomology, ICAR_ AINP on VPM, College of Agriculture and College of Forestry, Vellanikkara Thrissur, Kerala, for providing facilities and financial support for the study.

Funding declaration

Research funding and allocation was done by Kerala Agricultural University.

Author contributions

RSR initiated the study. RSR, RMT, MC, HER, VCV and KAG jointly designed the research. Data were collected by RSR and RSR, RMT, HER and KAG performed the data analysis. RSR drafted the initial version of the manuscript. RMT, MC, HER, VCV and KAG contributed to reviewing, editing, and revising the manuscript. All authors read and approved the final version for submission.

Declarations

Competing interest: The authors declare that no competing financial interests or personal relationships that could be appeared to influence this paper.

LITERATURE CITED

1. De Barro PJ, Liu SS, Boykin LM, Dinsdale AB. 2011. *Bemisia tabaci*: a statement of species status. *Annual Review of Entomology* 56: 1-19.
2. Misra H, Lambda V. 1929. First report of *Bemisia tabaci* in Punjab. *In*: historical cotton pest records.
3. Jiu M, Hu J, Wang LJ, Dong JF, Song YQ, Sun HZ. 2017. Cryptic species identification and composition of *Bemisia tabaci* (Hemiptera: Aleyrodidae) complex in Henan Province, China. *Jr. Insect Science* 17(3): 78.
4. Oliveira MRV, Henneberry TE, Anderson P. 2001. History, current status and collaborative research projects for *Bemisia tabaci*. *Crop Protection* 20(9): 709-723.
5. Horowitz AR, Ghanim M, Roditakis E, Nauen R, Ishaaya I. 2020. Insecticide resistance and its management in *Bemisia tabaci* species. *Journal of Pest Science* 93(3): 893-910.
6. Butter NS, Dhawan AK .2021. A monograph on whiteflies. CRC Press, Boca Raton, USA.
7. Government of Kerala. 2023. *A Compendium of Agricultural Statistics: Kerala 2023.* Directorate of Agriculture, Government of Kerala, Thiruvananthapuram.
8. Sivalingam PN, Varma A. 2007. Role of whitefly (*Bemisia tabaci*) in the transmission of Brinjal yellow mosaic virus in eggplant. *Journal of Plant Pathology* 89(2): 183-188.
9. Singh AK, Mishra R, Chattopadhyay B, Chakraborty S. 2016. Tomato leaf curl New Delhi virus: a begomovirus causing epidemics in vegetable crops. *Molecular Plant Pathology* 17(9): 1499-1512.
10. Gill RJ, Brown JK. 2010. Taxonomy and systematics of *Bemisia tabaci*: morphological approaches. *Journal of Insect Science* 17(4): 301-309.
11. Yan F. 2001. Morphology-based identification in the *Bemisia tabaci* complex. *Entomological Review* 81(5): 521-528.
12. Li R, Liu SS, De Barro PJ, Xu J, Zang LS, Zhang G. 2013. Comparative morphometrics of *Bemisia tabaci* puparia to distinguish biotypes. *Journal of Economic Entomology* 106(5): 2130-2138.
13. Harish ER, Chellappan M, Kumar TM, Ranjith MT, Ambavane AR. 2016. Morphometric variations in cassava (*Manihot esculenta* Crantz) whitefly *Bemisia tabaci* (Gennadius) (Hemiptera: Aleyrodidae) from different agro-ecological zones of Kerala, India. *Journal of Root Crops* 42(2): 90-102.
14. Peng J, Lv XL, Ran XT, Jindal V, Banta G, Gupta VK, Kumar V, Wu QJ, Mohindru B, McKenzie CL, Osborne LS. 2025. Geographical distribution and genetic analysis reveal recent global invasion of whitefly *Bemisia tabaci* primarily associated with only three haplotypes. *Bulletin of Entomological Research* 115(2): 194-206.
15. Legg JP, Jeremiah SC, Obiero HM, Maruthi MN, Ndyetabula I, Okao-Okuja G, Bouwmeester H, Bigirimana S, Tata-Hangy W, Gashaka G, Mkamilo G, Alicai T, Kumar PL. 2014. Comparing the regional epidemiology of the cassava mosaic and cassava brown streak virus pandemics in Africa. *Virus Research* 186: 61-70.
16. Navas-Castillo J, Fiallo-Olivé E, Sánchez-Campos S. 2011. Emerging virus diseases transmitted by whiteflies. *Annual Review of Phytopathology* 49: 219-248.